Hindawi
Advances in Civil Engineering
Volume 2020, Article ID 8875912, 12 pages
https://doi.org/10.1155/2020/8875912

Research Article

Test and Analysis of Sludge Dewatering with a Vacuum Negative Pressure Load at the Bottom of Full Section

Yongzheng Qi,[1] **Zongzhi Wang**,[2] **Pengming Jiang**,[1] **Yunfei Guan**,[2] **Liyan Wang**,[1] **Ling Mei**,[1] **Aizhao Zhou**,[1] **Heying Hou**,[1] **and Haoqing Xu**[1]

[1]*School of Civil Engineering and Architecture, Jiangsu University of Science and Technology, No. 2 Mengxi Road, Zhenjiang 212003, China*
[2]*State Key Laboratory of Hydrology-Water Resources and Hydraulic Engineering, Nanjing Hydraulic Research Institute, Nanjing 210029, China*

Correspondence should be addressed to Zongzhi Wang; wangzz77@163.com

Received 29 July 2020; Revised 13 September 2020; Accepted 29 September 2020; Published 14 October 2020

Academic Editor: Qiang Tang

At present, the sludge production has increased sharply, and sludge treatment remains a serious problem. Rapid sludge dewatering is the key problem of sludge treatment, and the main approach for reducing the cost of the sludge treatment is to reduce the cost of sludge dewatering. In this paper, two groups of sludge dewatering tests were carried out using homemade instruments and equipment. One group was conducted without rice straw, and the other group was conducted with rice straw. The relevant mechanism was analyzed, and the results indicate that sludge dewatering with a vacuum negative pressure load of the full section at the bottom is better than mechanical sludge dewatering. The sludge dewatering effect with rice straw is better than that without rice straw. Additionally, the vacuum degree inside the sludge decreased sharply. The pore water pressure slowly dissipates during the early and late stages and quickly during the middle stage. Sludge pore water seepage does not obey Darcy's law, and sludge dewatering is intermittent.

1. Introduction

At present, the sludge treatment situation in China's sewage treatment plants is severe, the sludge treatment capacity has increased sharply, and the sludge output will exceed 60 million tons in 2020 [1]. If the mud is not treated in a timely manner, it will cause secondary pollution to the environment. The moisture content of sludge is as high as 98% [2]. Studies have shown that if the moisture content of sludge is reduced from 99.3% to 60%~80%, then the volume can be reduced to 1/10~1/15 of the original volume, which can greatly reduce the cost of sludge transportation and further treatment [3]. In general, the cost of sludge treatment is up to 50%–60% of the construction and operation cost of the whole sewage treatment plant [4]. According to the interaction between water molecules and sludge solid particles, the water in sludge can be divided into free water, interstitial water, surface water, and internal binding water [5, 6], as shown in Figure 1. Among them, free water is not restricted by solid particles, interstitial water exists in the gap between the sludge flocs and organic matter, surface adsorbed water is adsorbed on the surface of sludge particles, and internal bound water is bound in organic matter cells through chemical bonds. Sludge dewatering is a solid-liquid separation process. Free water, interstitial water, and surface adsorbed water are the main objects of sludge dewatering and concentration, as shown in Figure 2. Sludge dewatering mainly includes natural dewatering and mechanical dewatering.

Natural drying is the earliest sludge dewatering process. Due to the influence of weather, time, and other factors, dewatering is difficult, and the effect is not ideal. Currently, mechanical dewatering is the main sludge dewatering method, such as belt filter press dewatering, plate and frame filter press dewatering, centrifugal dewatering, and stacked screw dewatering [7–9]. After the concentration or

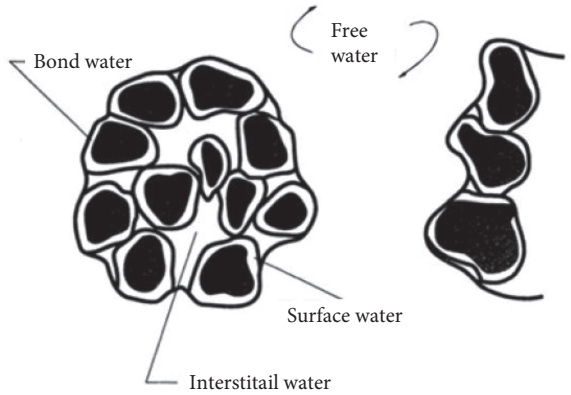

Figure 1: The moisture distribution in sludge [5].

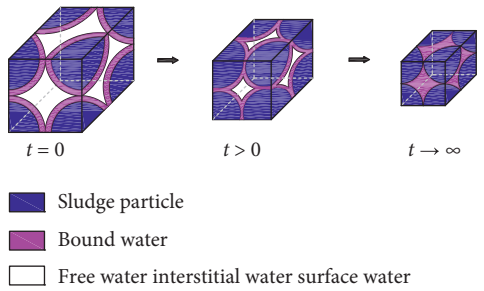

Figure 2: The process of sludge dewatering.

mechanical dewatering process, the lowest moisture content is still approximately 80% [10]. The moisture content required for the direct landfill of sludge is less than 60% and that required for the direct incineration of sludge is less than 50% [11]. To further reduce the moisture content of sludge, sludge is usually conditioned and modified before mechanical dewatering. Sludge conditioning methods mainly include chemical methods, physical methods, and microbial methods [12–14]. Regardless of which method is adopted, the cost of sludge treatment is relatively high.

In fact, sludge dewatering and soft soil drainage consolidation are essentially the same; both of them are the water discharge processes from the drainage channel driven by external forces. The sludge dewatering process [15] is shown in Figure 2, and the consolidation process of vacuum preloading drainage [16, 17] is shown in Figure 3. The vacuum preloading drainage consolidation method has been widely used in many projects [18–21], and the vacuum preloading method has been gradually introduced into sludge treatment in sludge landfills for sludge drainage and consolidation treatment [22–24]. However, the largest problem of vacuum preloading drainage and consolidation is that the drainage channel is silted up. The permeability of the filter membrane of the drainage plate is reduced, which reduces the drainage consolidation efficiency and weakens the drainage consolidation effect [25, 26]. In fact, sludge dewatering faces the same problem of silting and blocking due to the characteristics of the sludge solid particles, such as high hydrophilicity, difficult settling, and strong compressibility. In this paper, starting from the problem of sludge dewatering, the consolidation method and theory of vacuum preloading drainage are introduced for sludge dewatering. Additionally, model tests of sludge rapid dewatering with a vacuum negative pressure load at the bottom of the full section were carried out. The dewatering mechanism was analyzed.

2. Tests

A homemade rapid sludge dewatering system for providing a vacuum negative pressure load was adopted in the model tests, which included a sludge water separation box, an air-water separation device, a vacuum negative pressure power source, and a connecting pipe, as shown in Figure 4. The model box was made of transparent acrylic material. The internal net size of the box was 80 cm × 80 cm × 80 cm, and the wall thickness was 2 cm. The bottom of the model box was set as a hollow space, on which there was a transparent acrylic partition. The partition had 4 cm spacing and 1 cm diameter holes. From the bottom to the top, the slurry separation box consisted of a hollow space, permeable geotextile, a crop straw percolation layer, a sludge layer, and a vacuum sealing membrane.

First, a layer of permeable geotextile was laid on the diaphragm plate of the hollow space in the model box, and then crop straws were laid on the geotextile. The sludge was discharged onto the crop straws, and the sludge surface was covered with the sealing membrane. The hollow space at the bottom of the model box was connected with the air-water separation device through the sealing pipe, and the air-water

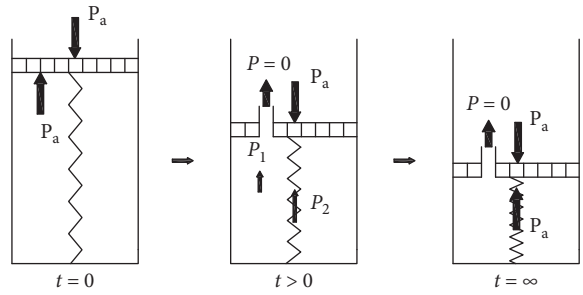

Figure 3: Spring piston model of vacuum preloading drainage consolidation [17].

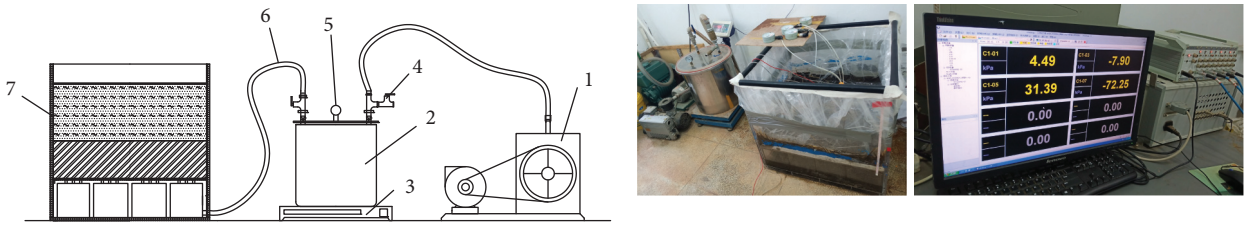

(a) (b)

Figure 4: Rapid sludge dewatering system with a vacuum negative pressure load at the bottom of the full section. (a) Schematic diagram of test model system. 1, vacuum pump; 2, gas-water separator; 3, electronic scale; 4, valve; 5, vacuum gauge; 6, connecting pipe; and 7, model box. (b) Test model pictures.

separation device was connected with the vacuum pump. The vacuum pump was vacuumed through the air-water separation device. The air-water mixture in the bottom overhead layer exerted a vacuum negative pressure load at the bottom of the model box.

The sludge was evenly stirred, and the initial moisture content of the sludge was measured. To test the effect and performance of sludge dewatering under vacuum negative pressure conditions at the bottom of the full section, the tests were divided into two groups: sludge dewatering without straw and sludge dewatering with rice straw.

For sludge dewatering without straw, the layer of permeable geotextile was laid on the diaphragm plate as the filter membrane. The edge of the geotextile was pasted and sealed with adhesive tape on the inner side of the box wall. The parameters of the permeable geotextile are shown in Table 1. The sludge was discharged onto the permeable geotextile. The thickness of the sludge was 30 cm. The upper surface of the sludge layer was covered with the sealing membrane and sealed with the four walls of the model box.

For sludge dewatering with rice straw, the nonwoven permeable geotextile and rice straw were selected as the permeable layer. The straw was acquired from local rice straw. The dry rice straw was orderly spread on the permeable geotextile as the percolation layer. A steel mesh with a weight of 20 kg as the precompression stress was applied to the rice straw, and the thickness of the rice straw layer was 10 cm. The vacuum monitoring points and the micropore water pressure gauges were embedded in the straw percolation layer. The sludge was discharged into the model box until the thickness of the sludge reached 30 cm. The vacuum monitoring points and the micropore water pressure gauges were buried inside the sludge and on the upper surface of the sludge, respectively. The embedded position of each sensor is shown in Figure 5. The upper surface of the sludge layer was covered with the sealing membrane.

The scale was set on the outer wall of the transparent model box to monitor the changes in the sludge layer thickness and straw percolation thickness with time. The gas-water separator was placed on the precise electronic scale to measure the water of sludge dewatering.

After the test preparation, the vacuum pump was started, and the test data were recorded. When there was no obvious change in the readings of sludge dewatering for two consecutive cycles, the test was terminated, and the sludge sample was taken to measure the final moisture content of the sludge.

3. Test Results and Analysis

3.1. Vacuum Negative Pressure Load at the Bottom of the Box. In the test, the whole section vacuum negative pressure load was applied to the sludge from the bottom of the box. The vacuum negative pressure load was basically maintained at 87–90 kPa and 90 kPa at the early stage of the test and slightly reduced at the later stage, maintaining at 87 kPa for the test with rice straw, as shown in Figure 6.

The vacuum negative pressure load at the bottom of the model of the sludge dewatering test without straw is 90 kPa, as shown in Figure 7.

3.2. Sludge Dewatering Rate. The sludge dewatering rate n_w reflects the degree of discharged water from the sludge, which is equal to the ratio of the mass ΔM_w of discharged

Table 1: Parameters of the permeable geotextile.

Aperture (mm)	Thickness (mm)	Surface density (g/m^2)	Permeability coefficient k_v (cm/s)
0.071	5.21	613	0.312

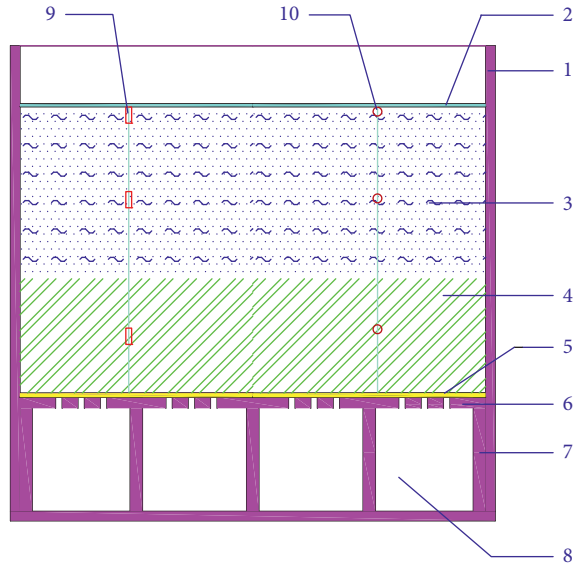

Figure 5: The test model and the monitoring points. 1, model box; 2, sealing membrane; 3, sludge; 4, straw; 5, permeable geotextile; 6, diaphragm plate; 7, support; 8, hollow space; 9, pore pressure gauges; and 10, vacuum monitoring points.

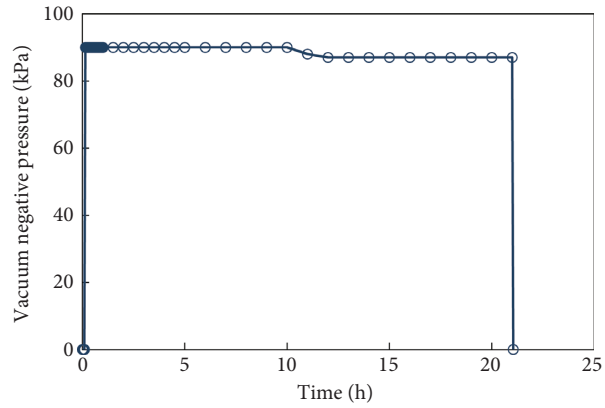

Figure 6: The vacuum negative pressure load of sludge dewatering with rice straw.

water at time t to the mass M_{w0} of the sludge water at the initial time, as shown in

$$n_w = \frac{\Delta M_w}{M_{w0}} = \frac{M_{w0} - M_{wt}}{M_{w0}} = \frac{M_{w0} - M_{wt}}{w_0 M_0}, \quad (1)$$

where M_0 is the total mass of the initial sludge solid particles and water, M_{wt} is the mass of water in the sludge at time t, and w_0 is the initial moisture content of the sludge.

The sludge dewatering rate with rice straw under a vacuum negative pressure load at the bottom of the full section is shown in Figure 8. The maximum dewatering rate is 93.3% in the 21-hour test. It can be seen from Figure 8 that the sludge dewatering is large in the early stage, and the dewatering is small in the later stage and then trends to the dewatering limit.

The sludge dewatering rate without straw is shown in Figure 9. The maximum dewatering rate is 94.25% in 48-hour test. According to the characteristics of the sludge dewatering rate, the curve of the sludge dewatering rate without straw under vacuum negative pressure of the full section at the bottom of the model is stepped, which indicates that sludge dewatering in this state is intermittent. In addition, it can also be seen that the sludge dewatering in the early stage is large, and the dewatering in the later stage is small.

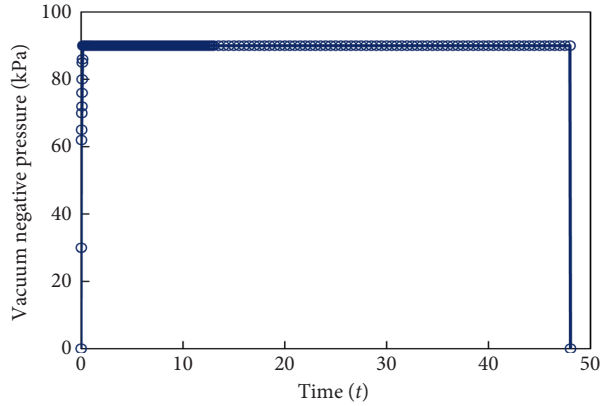

Figure 7: The vacuum negative pressure load of sludge dewatering without straw.

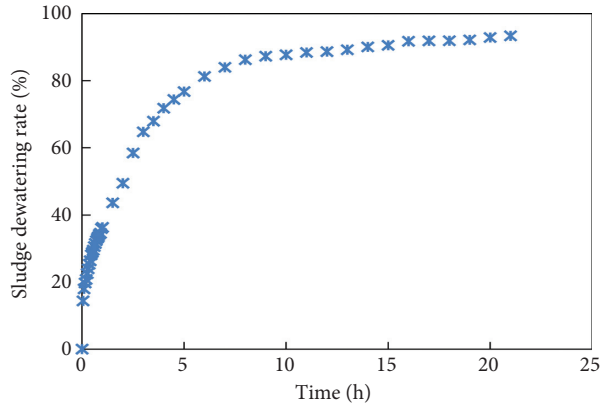

Figure 8: Sludge dewatering rate with rice straw.

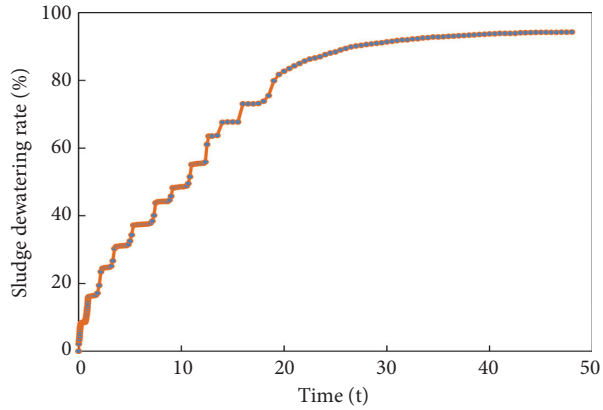

Figure 9: Sludge dewatering rate without straw.

3.3. Sludge Volume Concentration Rate. The sludge volume concentration rate refers to the degree of the sludge volume concentration at a certain time, which is equal to the difference between the initial sludge volume V_0 and the sludge volume V_t at time t divided by the initial sludge volume V_0. As the cross-sectional area of the model box is constant, the volume concentration rate is equal to the difference between the initial sludge thickness H_0 and the sludge thickness H_t at time t divided by the initial sludge thickness H_0. The calculation equation is shown in

$$n_v = \frac{V_0 - V_t}{V_0} = \frac{H_0 - H_t}{H_0}, \quad (2)$$

where H_0 is the initial sludge surface height and H_t is the sludge thickness at time t.

The volume concentration rate is shown in Figure 10. The maximum volume concentration rate is 91.6%. Figure 10 shows that the sludge dewatering volume concentration in the early stage is faster than that in the later stage. The volume after sludge dewatering and concentration is only 8.4% of the initial volume of sludge.

3.4. Moisture Content of Sludge. The moisture content of sludge w is the ratio of the mass of water in sludge M_w to the total mass of sludge solid particles and water M. The equation for the sludge moisture content at time t is shown in

$$w_t = \frac{M_{wt}}{M_t} = \frac{M_{wt}}{M_{st} + M_{wt}}, \qquad w_t = \frac{M_{w0} - \Delta M_w}{M_0 - \Delta M_w} = \frac{w_0 M_0 - \Delta M_w}{M_0 - \Delta M_w}, \quad (3)$$

where M_0 is the total mass of the initial sludge solid particles and water, M_{wt} is the mass of the sludge water at time t, ΔM_w is the mass of the sludge discharge water at time t, and w_0 is the initial moisture content of the sludge.

The sludge moisture content with rice straw under vacuum negative pressure conditions at the bottom of the full section is shown in Figure 11. The initial moisture content of sludge before the test is 98.13%. The moisture content of sludge is reduced to 77.71% after the sludge dewatering test with a vacuum negative pressure load in 21 hours, which is better than conventional mechanical dewatering result without sludge conditioning (80%).

The moisture content of the sludge without straw under a vacuum negative pressure load of the full section at the bottom of the model is shown in Figure 12. The initial moisture content of the sludge is 98.13%. The moisture content of the sludge after dewatering without straw under vacuum pressure for 21 hours is 89.18%, which is higher than that of the sludge with rice straw for 21 hours. The moisture content of the sludge is reduced to 75.1% after the sludge dewatering test in 48 hours. It is shown that the effect of sludge dewatering with rice straw is better than that of sludge dewatering without rice straw.

3.5. Vacuum Monitoring. Three groups of vacuum monitoring points (see Figure 5 for details) were set on the upper surface of the sludge, inside of the sludge, and inside of the straw percolation layer. The time curve of the vacuum monitoring points is shown in Figure 13. From the time curve of the vacuum degree, it can be seen that there is no change in the value of the vacuum degree on the upper surface of the sludge, and the vacuum degree in the sludge layer and straw layer lags behind the start time of vacuumizing for 6–8 hours. The vacuum degree inside the sludge decreased sharply.

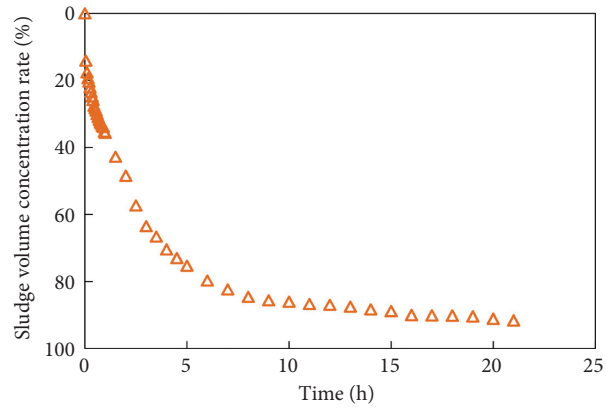

Figure 10: Sludge volume concentration rate.

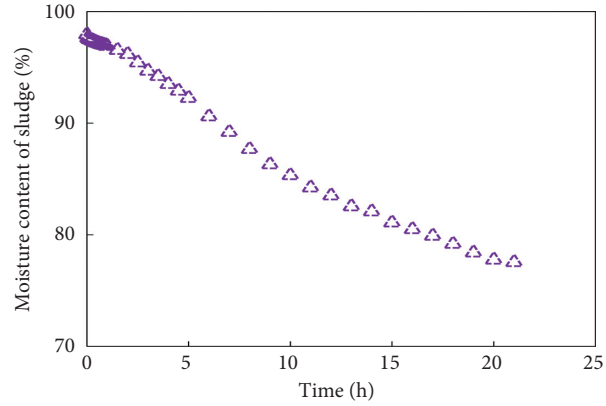

Figure 11: Sludge moisture content with rice straw.

3.6. Pore Water Pressure Monitoring. Three groups of pore water pressure gauges (as shown in Figure 5) were set on the upper surface of the sludge layer, inside of the sludge, and inside of the straw percolation layer, which are consistent with the position of the vacuum degree probes. The pore water pressure of the monitoring points is shown in Figure 14. From the curve of the pore water pressure at the monitoring points, it can be seen that the law of dissipation and the transmission of the negative excess pore water pressure in the sludge are very obvious. The dissipation is slow in the early and late stages and fast in the middle stage. The dissipation inflection point appears in the middle stage. The absolute value of the negative pore water pressure in the sludge is large at the bottom of the model and small in the upper part. The negative pressure transfers gradually from the bottom of the model to the upper part of the sludge.

4. Mechanism Analysis

4.1. Seepage Characteristics of Sludge Pore Water. The sludge particles have high hydrophilicity, and the layer of the water film is adsorbed on the surface of the sludge particles [27]. The water film on the surface of the particles is composed of a stern layer, a diffusive layer, and a bulk solution in sequence [28], as shown in Figure 15.

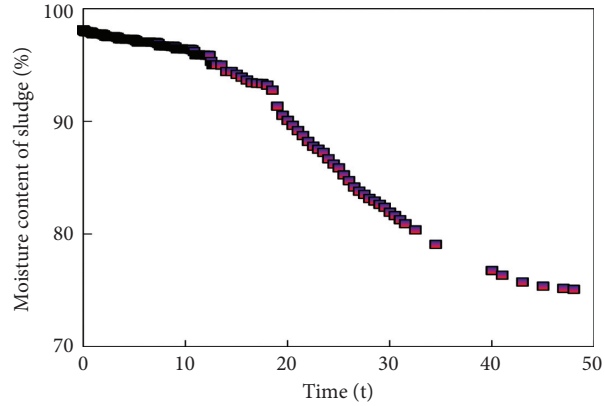

Figure 12: Sludge moisture content without straw.

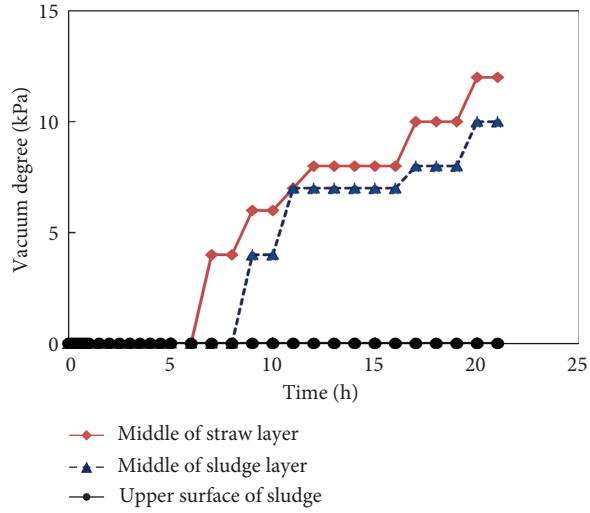

Figure 13: The vacuum degree at the monitoring points.

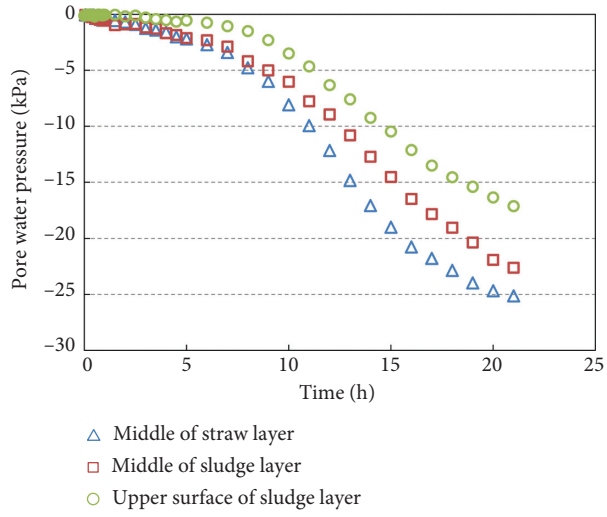

Figure 14: The pore water pressure at the monitoring points.

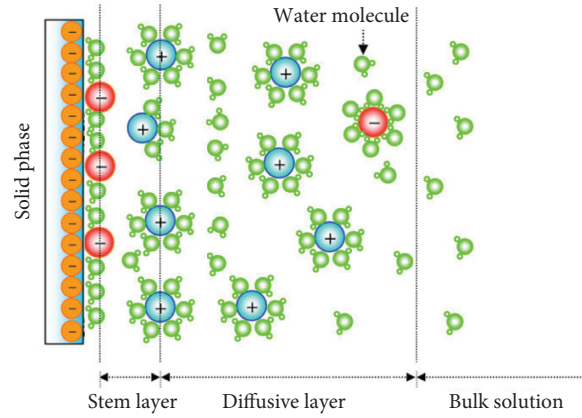

Figure 15: Schematic diagram of the water film on the surface of the sludge particles [28].

Sludge particles flocculate and settle under the action of a vacuum negative pressure load at the bottom of the section and form a layer on the surface of the straw layer. Due to the high-pressure shrinkage of sludge solids, the free water in the sludge pores is discharged under the action of a vacuum and negative pressure. The sludge volume is concentrated and deformed, and the pores are narrowed. The surface of sludge particles combined with the water film gradually occupies the seepage pores between the sludge particles, and thus, seepage will not occur. With an increase in the water head, the pore water pushes away the blockage of the combined water film, and seepage occurs again, as shown in Figure 16(a).

It can be seen that the seepage of pore water in sludge does not obey Darcy's law. There is an initial hydraulic gradient i_0 in the seepage, as shown in Figure 16(b). When the hydraulic gradient $i < i_0$, the bound water film in the pore restricts the flow of free water between the pores, and the pore water in the sludge does not seep at this time. When the hydraulic gradient rises gradually to i_0, the diffusive layer water is converted into free water and flows in the pores under the effect of the pore water pressure. The pore water overcomes the initial hydraulic gradient i_0, and seepage begins. When the hydraulic gradient $i > i_0$, the seepage velocity v and hydraulic gradient i of pore water in the sludge approximately meet Darcy's law. Therefore, for low-permeability porous media, the seepage of pore water has non-Darcy characteristics. According to the curve of the sludge dewatering rate without straw under vacuum negative pressure conditions at the bottom of the model, as shown in Figure 9, sludge dewatering is intermittent, which indicates that pore water needs to overcome the initial hydraulic gradient i_0 again and again for sludge seepage. The seepage of pore water in sludge is non-Darcy seepage.

4.2. Vacuum Degree and Pore Water Pressure. Sludge is a kind of porous media. The pores in sludge are composed of different sizes of pores, which are full of water and gas. At the beginning of vacuumizing, the gas in the bottom layer of the box is first pumped out to form a vacuum. The water and gas in the larger connecting channels close to the sludge in the straw percolation layer are sucked out due to the pressure difference and are connected gradually to the smaller channels in the sludge. At this time, the discharged water is mainly free water distributed in the sludge pores. The water level on the sludge surface drops, which changes the vertical self-weight stress in the sludge. The water in the finer pores of the sludge bears the negative excess pore water pressure and is discharged gradually, resulting in consolidation. Due to the "water sealing" effect caused by the existence of free water, the vacuum degree in the lower part of the sludge layer cannot easily diffuse to the upper part of the sludge layer, as shown in Figure 13. The sealing membrane floats on the upper surface of the sludge layer in the early stage of vacuumizing, and the sealing membrane clings to the upper surface of the sludge layer in the later stage. This behavior indicates that the vacuum degree is isolated in the lower part due to "water sealing" in the early stage and the "vacuum fluid" displaces the water in the cake pores in the later stage. The seepage path is opened in the sludge through the "finger in" function. The effect of the "finger in" branches gradually approaches the upper part of the sludge and reaches the lower part of the sealing membrane. The sealing membrane is adsorbed on the surface of the sludge, and then the sludge is extruded for dewatering.

The dissipation of the pore water pressure reflects the degree of sludge dewatering and consolidation. From the curve of the pore water pressure in Figure 14, it can be seen that sludge dewatering and consolidation expands gradually from the sludge bottom to the sludge surface near the sealing membrane. At the same time, it can be seen that the dissipation of the negative excess pore water pressure is slow in the early and late stages but fast in the middle stage. The dissipation inflection point appears in the middle stage. As shown in Figure 17, the pore pressure dissipation law in the traditional vacuum preloading drainage consolidation is fast in the early stage and slow in the later stage. The law is different from that of sludge dewatering under a vacuum negative pressure load at the bottom of the full section. As we know, the upper part of the traditional vacuum preloading is vacuumized, and the pore water is discharged from the upper surface. The pore water is rapidly discharged from the drainage channel at the initial stage of vacuumizing, which

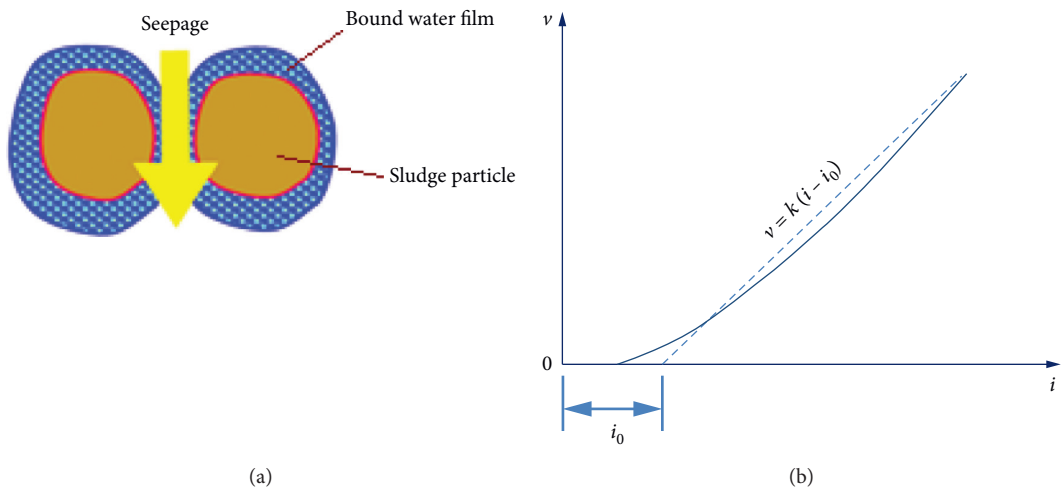

Figure 16: Sludge seepage model. i_0, initial hydraulic gradient; i, hydraulic gradient; v, velocity of permeability; k, coefficient of permeability.

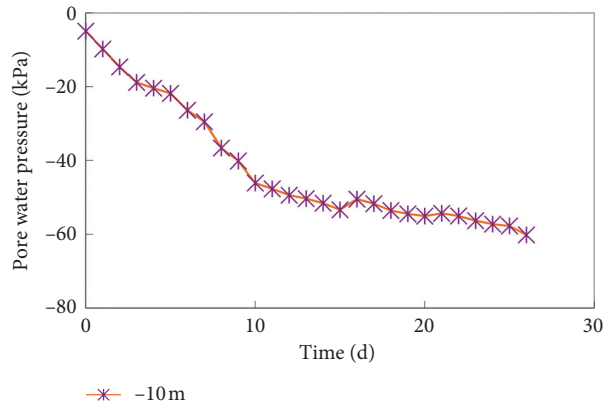

Figure 17: The excess pore pressure with traditional vacuum preloading (10 m underground).

causes the groundwater level to drop. The negative excess pore water pressure dissipates rapidly, and the pore water pressure is transformed into effective stress. Therefore, it is shown as the rapid dissipation of the pore water pressure in the early stage. The pore water is discharged slowly in the later stage of vacuum pumping, which shows that the pore water pressure dissipates slowly. For the bottom drainage under a vacuum negative pressure at the bottom, the sludge water needs to be discharged through the pores of the lower sludge cake. After the water in the pores of the lower sludge cake is discharged, it is supplemented by the water infiltrating continuously from the upper part. The pores are filled with pressure water, which is difficult to compress and thus cannot be easily converted into effective stress. Therefore, the early stage shows that the pore water pressure dissipates slowly, although the early stage of sludge dewatering is relatively fast. When there is no more excess pore water in the upper part of the sludge to infiltrate into the cake in the later stage, there is only the remaining water in the sludge to dehydrate slowly, which shows that the dissipation of the pore water pressure slows down again and tends to be stable gradually.

4.3. Sludge Dewatering Process and Mechanism of the Anti-clogging of Straw. As shown in Figure 10, the sludge volume concentration is faster in the early dewatering stage and slower in the later stage and tends to be stable. From the analysis of the interaction between sludge particles and water, this interaction produces a double electric layer. Under the action of the double electric layer, the sludge particles undergo flocculation, stratification, compression, and consolidation and finally form a high-density compressed sludge layer. From the point of view of porous media, the sludge dewatering process under a vacuum negative pressure load at the bottom of the full section can be divided into two stages. The first stage is the flocculation and deposition of sludge particles under self-weight and the seepage force generated by the vacuum negative pressure, as shown in Figures 18(a) and 18(c). The sludge particles are deposited into the interior and surface of the straw layer under continuous negative pressure, and a sludge cake is formed on the surface. A large amount of free water in the sludge pores is patted out and discharged from the bottom through the sludge cake and straw percolation layer. The sludge is rapidly dewatered, and the volume is sharply

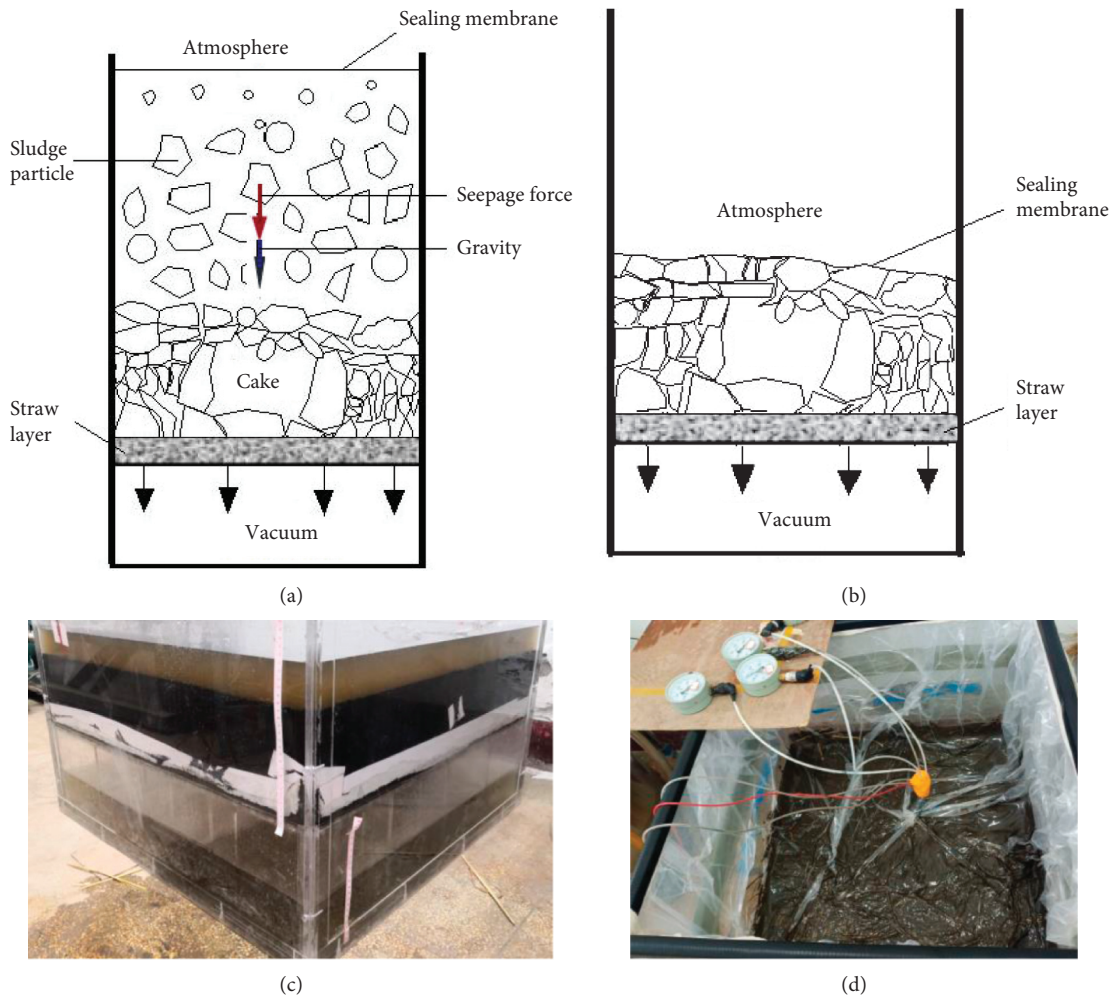

Figure 18: The deposition and consolidation process of sludge particles: (a) and (c), deposition of sludge particles; (b) and (d), gas-water conversion.

concentrated. The second stage is gas displacement dewatering under the action of negative pressure, as shown in Figures 18(b) and 18(d). Negative pressure gas passes through the pores of the sludge cake and displaces a small amount of free water, interstitial water, and part of the surface water in the sludge cake. At this time, the sludge dewatering is very slow, and the sludge cake becomes increasingly dense. Under the effect of negative pressure, the sludge cake is forced to press and filter, and the sludge cake is gradually dewatered and consolidated.

In the early stage of the experiment, due to the "water sealing" effect of free water, the pressure on the upper sealing membrane of the sludge surface did not play a role. The vacuum drainage of sludge mainly relies on the vacuum negative pressure applied at the bottom. The rice straw has a unique internal pore structure and certain adsorption characteristics, which makes part of the free water in the sludge absorbed by the rice straw, and the sludge flocculent body is blocked outside the straw fiber. The sludge flocculent forms a certain flocculation framework in the straw fiber gap. At this time, there are three states: permeable geotextile in the bottom layer, saturated crop straw in the middle, and flocculation framework formed by the sludge in the straw fiber gap. Due to the effect of the vacuum negative pressure at the bottom of the box, the water in the rice straw is continuously discharged through the permeable geotextile, and the missing water in the rice straw is supplemented from the outside of the flocculent skeleton. The drainage body of the rice straw filters water at first and then drains water from the permeable geotextile. Because of the continuous drainage of rice straw, it is necessary to constantly absorb the water outside the framework of the flocs. In this process, the fine particles in the sludge will pass through the floc skeleton to the surface of the permeable geotextile and gradually form a fine particle sludge layer on the surface of the permeable geotextile with the passage of time. With the discharge of water, the volume of the sludge decreases, and the sludge is compressed under atmospheric pressure due to the sealing membrane. The effect of atmospheric pressure makes the straw drainage body compressed and deformed, and the framework of the sludge flocculent body is further squeezed. The free water, interstitial water, and part of the surface

water in the sludge cake are discharged under atmospheric pressure at the upper surface and vacuum negative pressure at the bottom.

The internal siltation of permeable geotextile becomes a slow sludge dewatering test with rice straw under a negative vacuum pressure load at the bottom of the full section due to the unique pore structure and adsorption characteristics of the rice straw. The air pressure compresses the sludge and rice straw, similar to the extrusion sponge body in the later stage of the test. The water that cannot be discharged under the bottom vacuum pressure is partially squeezed out, so the drainage effect is better.

5. Conclusion

Two groups of sludge dewatering tests were carried out using a homemade instrument and equipment. One group was conducted without rice straw, and the other group was carried out with rice straw. The relevant mechanism of rapid sludge dewatering under negative vacuum pressure at the bottom of the full section was analyzed. The conclusions are as follows:

(1) The effect of sludge dewatering with a vacuum negative pressure load at the bottom of the full section is better than that of mechanical sludge dewatering. The sludge moisture content after dewatering can be reduced to less than 80% without sludge conditioning and modification.

(2) The effect of sludge dewatering with rice straw under vacuum negative pressure conditions is better than that without rice straw. Rice straw can improve sludge clogging effectively and benefit sludge dewatering.

(3) The vacuum degree inside of the sludge decreased sharply, and the pore water of the sludge has the function of "water sealing."

(4) The pore water pressure at the bottom of the sludge dissipates faster than that at the top of sludge, and it is transmitted from the bottom to the upper part. The dissipation of pore water pressure is slow at the early and later stages but fast at the middle stage.

(5) Sludge pore water seepage does not obey Darcy's law, and sludge dewatering is intermittent.

Data Availability

The data used to support the findings of this study are available from the corresponding author upon request.

Conflicts of Interest

The authors declare that they have no conflicts of interest.

Acknowledgments

The work described in this article was supported by the Key Laboratory of Ministry of Education for Geomechanics and Embankment Engineering (2019008), National Key Research and Development Program of China (2016YFC0800201), National Natural Science Foundation of China (51979128), Natural Science Foundation of Jiangsu Province (BK20190963), and Science and Technology Project for Construction System in Jiangsu Province (2018ZD093).

References

[1] C. Zhang and L. N. Sun, "Current situation and recycling development prospects of sludge treatment and disposal," *Heilongjiang Agricultural Sciences*, vol. 9, pp. 158–161, 2018.

[2] J. Fan, Q. Chen, J. Li et al., "Preparation and dewatering property of two sludge conditioners chitosan/AM/AA and chitosan/AM/AA/DMDAAC," *Journal of Polymers and the Environment*, vol. 27, no. 2, pp. 275–285, 2019.

[3] S. Nan and Y. Jia, "Experimental research of sludge dewatering by vacuum filtration," *Journal of Zhengzhou University*, vol. 35, no. 3, pp. 83–85, 2003.

[4] C. Ning, Z. Shengsheng, L. Jianhua et al., "A process in the dewatering of municipal sludge," *Guangdong Chemical Industry*, vol. 46, no. 16, pp. 138–140, 2019.

[5] K. R. Tsang and P. A. Vesilind, "Moisture distribution in sludges," *Water Science and Technology*, vol. 22, no. 12, pp. 135–142, 1990.

[6] F. Colin and S. Gazbar, "Distribution of water in sludges in relation to their mechanical dewatering," *Water Research*, vol. 29, no. 8, pp. 2000–2005, 1995.

[7] R. I. Dick, "Comment on "Experimental analysis of centrifugal dewatering process of polyelectrolyte flocculated waste activated sludge"," *Water Research*, vol. 36, no. 6, pp. 1649-1650, 2002.

[8] J. Li, "Dewatering experiment on three kinds of sludge from refineries," *Petrochemical Safety & Environmental Protection Technology*, vol. 29, no. 2, pp. 58–60, 2013.

[9] R. J. Wakeman, "Separation technologies for sludge dewatering," *Journal of Hazardous Materials*, vol. 144, no. 3, pp. 614–619, 2007.

[10] J. B. Liu, Y. M. Li, L. Jian et al., "Performance and factors analysis of sludge dewatering in different wastewater treatment processes," *Environmental Science*, vol. 36, no. 10, pp. 3794–3800, 2015.

[11] L. Hui, X. Wu, L. Jiang et al., "Progress on the dewatering and drying technology of municipal sludge," *Environmental Engineering*, vol. 32, no. 11, pp. 102–107, 2014.

[12] L. Jibao, W. Yuansong, L. Kun et al., "Microwave-acid pretreatment: a potential process for enhancing sludge dewaterability," *Water Research*, vol. 90, pp. 225–234, 2015.

[13] K. B. Thapa, Y. Qi, S. A. Clayton et al., "Lignite aided dewatering of digested sewage sludge," *Water Research*, vol. 43, no. 3, pp. 0–634, 2009.

[14] W. Yang, Q. Zhang, Q. Yang et al., "A review on municipal sludge dewatering and bioleaching conditioning technologies," *Industrial Water Treatment*, vol. 38, no. 4, pp. 11–16, 2018.

[15] L. Tang, Z. Luo, L. Zhang et al., "Research status and new views of sludge dewatering," *Technology of Water Treatment*, vol. 42, no. 6, pp. 12–17, 2016.

[16] Y. Qin and D. Cao, "Consolidation of soft soil foundation by vacuum-pumping in low level position," *Geoscience*, vol. 13, no. 4, pp. 471–476, 1999.

[17] J. Song, R. Y. Yue, and P. Zhang, "Analysis on mesoscopic dynamic of soft soil foundation in the pearl river delta region

based on the vacuum preloading method," *Advanced Materials Research*, vol. 594-597, pp. 100–104, 2012.

[18] W. Zhao, A. I. Ying, and J. Zhang, "Study on post-construction settlement of thick soft roadbed improved by drainage preloading," *Hydro-Science and Engineering*, no. 1, pp. 28–33, 2003.

[19] Q. I. Yong-Zheng and W. B. Zhao, "Study on theory of shear strength increment of soil body by draining consolidation for improving soft clay," *Hydro-Science and Engineering*, vol. 34, no. 2, pp. 78–83, 2008.

[20] X. U. Hong, X. J. Deng, Q. I. Yong-Zheng et al., "Development of shear strength of soft clay under vacuum preloading," *Chinese Journal of Geotechnical Engineering*, vol. 32, no. 2, 2010.

[21] N. D. Quang and P. H. Giao, "Improvement of soft clay at a site in the Mekong Delta by vacuum preloading," *Geomechanics and Engineering*, vol. 6, no. 5, pp. 419–436, 2014.

[22] X.-J. Zhan, W.-A. Lin, L.-T. Zhan, and Y.-M. Chen, "Field implementation of $FeCl_3$-conditioning and vacuum preloading for sewage sludge disposed in a sludge lagoon: a case study," *Geosynthetics International*, vol. 22, no. 4, pp. 327–338, 2015.

[23] F. Liu, W. Wu, H. Fu et al., "Application of flocculation combined with vacuum preloading to reduce river-dredged sludge," *Marine Georesources & Geotechnology*, vol. 38, no. 2, pp. 164–173, 2019.

[24] Z. Geng, Y. W. Jin, and G. Liu, "Application of vacuum preloading foundation treatment with air pressure boosted method to management of sludge storage landfill pit," *China Water & Wastewater*, vol. 34, no. 8, pp. 63–66, 2018.

[25] Q. Tang, F. Gu, Y. Zhang, Y. Zhang, and J. Mo, "Impact of biological clogging on the barrier performance of landfill liners," *Journal of Environmental Management*, vol. 222, pp. 44–53, 2018.

[26] T. Qiang, K. Heejong, E. Kazuto, K. Takeshi, and I. Toru, "Size effect on lysimeter test evaluating the properties of construction and demolition waste leachate," *Soils and Foundations*, vol. 55, no. 4, pp. 720–736, 2015.

[27] Q. Tang, W. Liu, Z. Li, Y. Wang, and X. Tang, "Removal of aqueous Cu(II) with natural kaolin: kinetics and equilibrium studies," *Environmental Engineering and Management Journal*, vol. 17, no. 2, pp. 467–476, 2018.

[28] A. Mahmoud, J. Olivier, J. Vaxelaire, and A. F. A. Hoadley, "Electrical field: a historical review of its application and contributions in wastewater sludge dewatering," *Water Research*, vol. 44, no. 8, pp. 2381–2407, 2010.